Extensive experimental validation of a model of pneumatic conveying drying for cassava starch

Arnaud Chapuis, Charlene Lancement, Francisco Giraldo, Léa Vand der Werf, Marcelo Precoppe, Dominique Dufour, Thierry Tran

ARTICLE HISTORY
Compiled November 7, 2021

Afilliation

Abstract
Main message: The model describes well the behavior of the process and can be used for equipment design and defining process control strategy (philosophy).

Originality: The paper presents the validation of a flash drying model, based on extensive experimental data collected on a pilot-scale pneumatic dryer.

1. Introduction

Cassava is a strategic agricultural value chain in many tropical countries, providing staple food products for an estimated 800 million people [1] and contributing to food security. In sub-Saharan Africa in particular, cassava consumption is typically between 100 and 250 kg/capita/year depending on the country, whereas in Europe and North America consumption of roots and tuber crops hovers around 60 kg/capita/year, mainly potatoes [2]. While cassava is well-liked for its tolerance to drought and ability to grow even in poor soils, its roots are highly perishable and start to spoil within 48 hours after harvest, through a process known as physiological post-harvest deterioration [3]. Post-harvest processing plays therefore a key role in transforming fresh roots quickly, either for direct consumption (e.g. as boiled cassava) or for extending shelf-life by producing dried products (e.g. gari, fufu flour, high-quality cassava flour, starch) that can be stored and commercialized over longer periods. Post-harvest processing determines the quality and food safety of cassava end-products. Beyond product quality, processing is also key in improving the sustainability of cassava value chains: by optimizing processing technologies, it is possible to reduce energy and water consumption, product losses, production costs, and the overall environmental footprint of cassava industries.

One of the main challenges facing smallholder farmers and small-scale entrepreneurs in processing cassava is drying. Many of them rely on sun-drying which limits processing during the rainy season as well as affects the overall quality. This is particularly limiting to access larger markets that need regular, all-year-round supply and consistent quality (IITA, 2016), such as high quality cassava flour (HQCF) and starch for the food industry (bakery, etc.). Pneumatic conveying drying (or flash drying) is a promising technology to enable substantial gains in productivity and quality of pow-

der products such as starch and HQCF. Its key advantages are reducing drying time from 10-48 hours (compared to sun-drying and tray drying) down to a few seconds, and ensuring constant drying conditions. Currently, flash dryers are used at large-scale (production capacity $>$ 50 tons product/day) in countries such as Thailand, Vietnam and Brazil. In contrast, small-scale flash dryers (1-3 tons product/day) are not used widely, due to a combination of factors including high energy consumption related to sub-optimal design, and consequently high production costs incompatible with market prices of final products (REF). Nevertheless small-scale flash dryers would be highly useful for economic development in countries where cassava value chains are not suitable for large-scale processing due to limited cassava supply, in order to meet increasing demand for long-shelf life products needed by growing urban populations.

To address this issue, we conducted research on the modeling of flash drying aiming to optimize the design of small-capacity flash dryers for energy efficiency. Article previously published in Drying Technology [4] presented a model for the pneumatic drying of cassava starch, whose originality was to consider the water diffusion within starch particles as the driving mechanism of drying kinetics. In absence of experimental data, the model outputs were confronted to data from five industrial-scale dryer to validate the consistency and order of magnitude of the results. As part of research and development activities conducted by CGIAR's research program on Roots, Tubers and Bananas (RTB), we developed a pilot-scale dryer (capacity 100 kg/h) at CIAT (Colombia) hat achieves similar energy efficiency as large-scale industrial flash dryers. We conducted extensive trials on this equipment to test and validate the drying model on a wide range of operating conditions, which is the object of the present paper. Finally, we analyzed the consequences of our findings on the strategy of design and operation of energy-efficient small-scale flash dryers.

2. Material and Methods

Based on a series of experiments conducted on a pilot-scale dryer, we investigated the capacity of the previously developed drying model to predict the behavior of the process under various operating conditions. First, the model parameters were fitted to experimental data from a series of drying runs under steady-state operation. Then, the model was tested for its ability to predict the dynamic response of the process to variations in the operating conditions. The response to a sudden change in feed rate was measured and simulated.

2.1. *Pneumatic drying model*

2.1.1. Model equations, hypotheses and solving method

The pneumatic drying model we aim to test and validate against experimental data in the present article was originally presented by [4]. In this section, we present only a brief reminder of the model equations and solving method while the full details are available in [4]. The model allows calculating the changes in temperature, moisture content, and velocity of air and starch particles along the drying pipe.

The main hypotheses of the model are the following:

- Plug flow, one-dimensional model: the conditions are radially homogeneous at a given position along the pipe.

- Particles are considered spherical, all of the same diameter, and their size is constant during drying (but their porosity increases). This assumption considerably simplifies the reality since the actual particle size distribution is not modeled, neither the attrition or agglomeration effects that could occur during drying. Therefore, the particle diameter was considered as a parameter of the model.
- Particle drying is diffusion-driven, meaning that the drying rate is determined by the diffusion of water within the solid particles, which is slow compared to the convective mass transfer at the particle surface.
- The water diffusivity of starch is isotropic but temperature- and moisture-dependent. Therefore, the diffusion equation was solved in one dimension, assuming central symmetry.
- Particle temperature is homogeneous.

The model consists of a system of conservation equations of heat, water and momentum transferred between the drying air and the particles. The momentum balance equations (Eq 1-2) describes the movement of air and starch particles. The initial air velocity u_a^0 is defined as the velocity of air right before the starch feed point. The initial starch particle velocity is set to value slightly higher than zero, here 0.5 $m.s^{-1}$, for convergence reasons.

$$\begin{aligned} &\frac{du_p}{dt} = \dot{u}_p = \frac{A'_p}{2V_p} \cdot C_D \cdot \frac{\rho_a}{\rho_p} \cdot (u_a - u_p) \cdot |u_a - u_p| \pm \left(1 - \frac{\rho_a}{\rho_p}\right) \cdot g - \frac{f_p \cdot {u_p}^2}{2D} \\ &u_p(t_0) = 0.5\ m.s^{-1} \end{aligned} \tag{1}$$

$$\begin{aligned} &\frac{du_a}{dt} = \dot{u}_a = -\frac{1}{\rho_a \cdot u_a} \cdot \frac{dP}{dt} \pm g - \frac{4 f_a \cdot {u_a}^2}{2D} - \frac{A'_p}{2V_p} \cdot C_D \cdot \frac{1-\epsilon}{\epsilon} \cdot (u_a - u_p) \cdot |u_a - u_p| \\ &u_a(t=0) = u_a^0 \end{aligned} \tag{2}$$

The porosity of the bed of particles ϵ is the ratio of the air volume to the total volume of air and particles at a given position along the pipe, according to equation 3.

$$\frac{\dot{m}_{da} \cdot (1+Y)}{\rho_a} = u_a \cdot S \cdot \epsilon \tag{3}$$

The heat balance in equations 4 and 5 describes the variations of air and particle temperature as a function of water evaporation and heat transfers.

$$\begin{aligned} &\frac{dT_p}{dt} = \frac{A_p}{V_p} \cdot \frac{1}{\rho_p \cdot C_{\mathrm{p},p}} \cdot (\dot{q} - \dot{w} \cdot L_s) \\ &T_p(t_0) = T_p^0 \end{aligned} \tag{4}$$

$$\frac{dT_a}{dt} = -\frac{1}{C_{\mathrm{p},a}} \cdot \left(\frac{A_p}{V_p} \cdot \frac{1-\epsilon}{\epsilon} \cdot (\dot{q} + \dot{w} \cdot C_{\mathrm{p},v} \cdot (T_a - T_p)) + \frac{\dot{Q}_{loss} \cdot u_a}{\dot{m}_{da} \cdot (1+Y)} \right)$$
$$T_a(t_0) = T_a^0 \tag{5}$$

The water mass balance (equations 6 and 7) describes the variations of starch and air moisture content.

$$\frac{dX}{dt} = \dot{X} = -\frac{A_p \cdot \dot{w}}{V_p \cdot \rho_p} \cdot (1+X)$$
$$X(t_0) = X_0 \tag{6}$$

$$\dot{Y} = -\dot{X} \cdot \frac{\dot{m}_{ds}}{\dot{m}_{da}}$$
$$Y(t_0) = Y_0 \tag{7}$$

At particle level, the drying rate was calculated by solving the water diffusion equation 8. At the particle interface, the continuity of water vapor pressure applies, then the corresponding water concentration was deduced from the starch sorption isotherm.

$$\frac{\partial C}{\partial t} = \frac{1}{r^2} \cdot \frac{\partial}{\partial r} \left(r^2 \cdot D_{ws}(C, T_p) \cdot \frac{\partial C}{\partial r} \right)$$
$$C(t_0, r) = C_0 \quad ; \quad p_v(t, R) = p_v(Y) \tag{8}$$

The convective heat flux between the drying air and a particle was calculated from equation 9.

$$\dot{q} = h_p \cdot (T_a - T_p) \tag{9}$$

Finally the heat losses to the ambient through the drying pipe wall were evaluated using equation 10 .

$$\frac{d\dot{q}_{loss}}{dz} = k_{loss} \cdot \frac{T_a - T_{amb}}{R_{th}}, with:$$
$$R_{th} = \frac{1}{h_{ext} \cdot P_{ext}} + R_{rw} + R_{ss} + \frac{1}{h_{in} \cdot P_{in}}$$
$$R_{ss} = \frac{1}{2\pi \cdot \lambda_{ss}} \cdot ln \left(\frac{r + th_{ss}}{r} \right)$$
$$R_{rw} = \frac{1}{2\pi \cdot \lambda_{rw}} \cdot ln \left(\frac{r + th_{ss} + th_{rw}}{r + th_{ss}} \right) \tag{10}$$

where $\dot{q}_{loss}[W]$ is the heat loss through the pipe wall, $z[m]$ is the position along the pipe, $k_{loss}[-]$ is a heat loss correction factor, $R_{th}, R_{ss}, R_{rw}[K \cdot m \cdot W^{-1}]$ are respectively the total thermal resistance between the inside of the pipe to the ambient, the thermal resistance of the stainless steel pipe and of the rockwool insulation. $h_{ext}, h_{in}[W \cdot m^2 \cdot K^{-1}]$ are the external and internal heat convection coefficients respectively, $P_{ext}, P_{in}[m]$ are the external and internal perimeter, $\lambda_{rw}, \lambda_{ss}[W \cdot m^{-1} \cdot K^{-1}]$ are the thermal conductivity of rockwool and stainless steel, $r[m]$ is the internal radius of the drying pipe, $th_{ss}, th_{rw}[m]$are the thickness of the stainless steel pipe and of the rockwool insulation.

The model was implemented using Matlab® software (MathWorks, Natick, MA). The mass, momentum, and energy balance equations are solved using a fourth-order Runge–Kutta integration method. At each time step, the convective heat flux from the air to the particle is calculated and the drying rate is calculated by solving the water diffusion equation using the finite difference explicit method, using a discretization scheme recommended by Ford Versypt and Braatz (2014). Full details about the implementation of the model as well as the properties used for starch and moist air are available in [4].

2.1.2. Fitting parameters

To fit the model output to the experimental results, two parameters were adjusted: the heat loss correction factor and the particle diameter. As presented in equation 10, the heat losses through the dryer's wall were estimated using a heat transfer calculation with thermal resistances in series including internal convection, conduction through the insulation and external convection to ambient. This method gives a valuable estimate of the order of magnitude of the losses but needs adjustment to account for inaccuracies in heat transfer correlations, neglected phenomenon (e.g. heat transfers at flanges and feeding zones, radiations) and variable ambient conditions (e.g. wind velocity, air humidity). To this purpose, a correcting, factor k_{loss}, was included in the equation.

In the drying model, the description of the starch particles' size and shape was highly simplified (spherical, equal and constant diameter). Therefore, the particle diameter was considered as a parameter, representative of a more complex physical reality, i.e. size distribution, non-spherical shape and possible attrition or agglomeration effects. The initial particle size of the starch may be primarily affected by the characteristics of cassava roots and the starch production process. In the present work, the starch was produced from a unique cassava variety and by the same factory, therefore the initial characteristics of the product were assumed to be homogeneous. Then, during drying, the evolution of the particle size distribution of the starch may be affected by many factors including its initial moisture content, the dryer's feeding system (disaggregator) and the operating conditions, especially the air velocity and temperature. Researches on pneumatic conveying have highlighted that particle fragmentation and attrition were mostly conditioned by air velocity and conveying length [5, 6, 7]. In pneumatic conveying drying, air temperature and initial moisture content, to a lesser extent, may also affect the agglomeration of starch particles, as demonstrated by [8]. Therefore, the variations of the fitted particle diameter were analysed with respect to the dryer's operating conditions.

2.2. *Experimental materials and methods*

2.2.1. Pilot-scale flash dryer description

The pneumatic dryer used for the experiments was built at the CIAT's premises in Cali, Colombia and is presented in Figure 1 . It was designed for a capacity of 50-150 kg/h of wet product. The drying pipe was 15 cm in diameter and adjustable in length from 17 to 27 meters. It had a fixed vertical section with a bend at the top at about 7 m from the product feed point, followed by a horizontal section, where pipe portions could be added or removed to change the total length. The suction fan and the cyclone separator were mounted on mobile skid so they could be moved according to the chosen length.

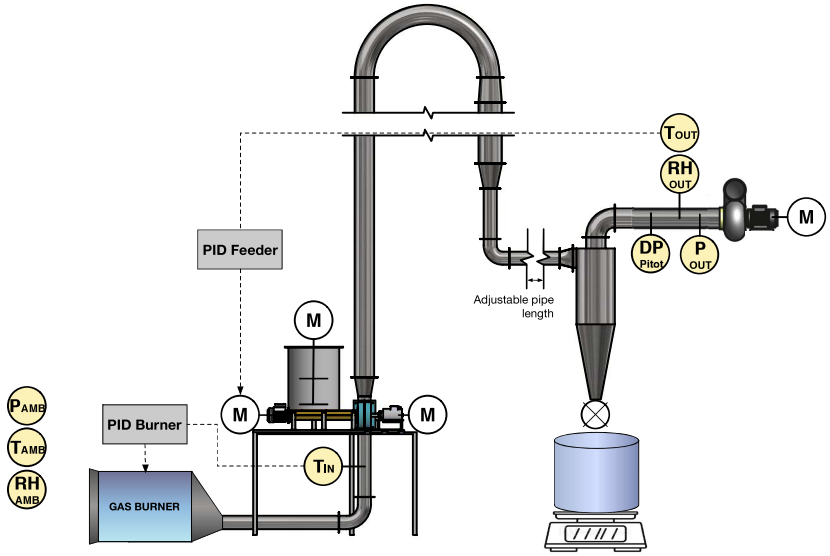

Figure 1.: Process and instrumentation diagram of the pilot flash dryer. All sensors and the balance are connected to a data acquisition system. (T = Temperature, P = Pressure, RH = Relative humidity, DP = Differential pressure).

The centrifugal fan was powered by a 5.5 kW electric motor through a variable-frequency drive allowing the adjustment of air velocity from 10 to 26 m.s^-1. The drying air was directly heated by a gas burner set at the pipe inlet delivering a thermal output of 10 to 90 kW. The heating system was controlled by a PID controller, allowing the adjustment of drying air inlet temperature between 130 and 200 °C.

Wet cassava starch is a sticky product, therefore the feeding system was designed to avoid the formation of bridges and ensure the pulverization of the product. It was composed of a cylindrical stirred hopper discharging in a screw conveyor leading the wet product to a pin mill connected to the drying pipe. The pin mill rotating at 2 000 rpm ensured the disaggregation of the product into fine particles. Given the low flowability of wet starch, the mass flowrate cannot be controlled simply by adjusted the screw-feeder rpm. Instead, the feed rate was controlled by a PID controller that adjusted the screw conveyor rotational speed to regulate a constant temperature of the exhaust drying air. This control strategy is commonly implemented on industrial dryers and enables a stable operation of the process.

The system's instrumentation monitors all the parameters required for mass and

energy balance assessment. Sensor measurements were recorded by a data acquisition system Almemo 710 (Ahlborn GmbH, Holzkirchen, Germany) at a frequency 1Hz. Air temperature was measured at the dryer inlet before the feed point and the outlet, after the cyclone, using 3 mm RTD probes. Two capacitive RH-meters FHAD36 (Ahlborn GmbH, Holzkirchen, Germany) were installed in the ambient and at the dryer's outlet, after the cyclone. Atmospheric pressure was measured from the pressure sensor embedded the Almemo data logger and the process pressure at the cyclone outlet was measured by a pressure sensor FDAD35M01A (Ahlborn GmbH, Holzkirchen, Germany). A Pitot tube connected to a differential pressure sensor FDA602S1K (Ahlborn GmbH, Holzkirchen, Germany) was installed in a straight pipe section at the cyclone outlet and after a flow stabilizer to provide the air velocity. The dried product discharged from the cyclone through a rotary airlock valve was collected into a tank placed on a scale Ohaus ES200L (Ohaus, Nänikon, Switzerland), also connected to the data acquisition system.

2.2.2. Drying material

Food-grade cassava roots were obtained from experimental fields at CIAT (Cali, Colombia) and from commercial producers in the Cauca (Colombia). Starch was extracted at a small-scale cassava processing factory located in la Agustina (Cauca department, Colombia), in batches of 1 ton of cassava roots. After extraction, starch was sedimented overnight in sedimentation canals [9] to reach a moisture content between 45 and 50% (wb).

In commercial settings, prior to flash-drying, starch undergoes a dewatering step to reduce moisture content as much as possible (typically 35% wb) by mechanical means such as filter-centrifugation or pressing, in order to reduce fuel consumption at the drying step. In absence of a suitable dewatering equipment for the processed capacity, wet starch was pre-dried by spreading it on plastic sheets under the sun. It took typically one day (9am to 4pm) to reach moisture content of 34-37% wb. After sun drying, the starch from a same batch (typically 100-150 kg) was mixed and packed in 20-kg polythene bags and stored in a cold room (4°C) for at least three days to let moisture content equilibrate inside each bag.

The main drawback of this pre-drying method was that it was difficult to aim for an accurate moisture content. Nevertheless, in order to vary the product input moisture in the drying experiments, the pre-drying time of the starch batches was varied to get moisture content in the low range (31-33%) and high range (36-38%). For each drying experiment a batch of wet starch of 100-150 kg with homogeneous moisture was prepared by mixing several bags and stored for a few days in a cold room for equilibration. Moisture variability in a batch was tested by oven drying 5 samples for 24 hours at 105°C and kept below +/- 2 % relative to the mean measured value.

2.2.3. Experimental plan and procedure

Two kinds of drying experiments were conducted:

- (i) operation in steady state, under various operating conditions and drying length.
- (ii) transient phase between two operating regimes in response to a step change of the set-value of the air outlet temperature on the feeder's PID controller, which induces a change of product feed rate.

A total of 52 drying runs were conducted in steady-state operation. The effects of various drying conditions were studied, including the drying air inlet velocity and temperature and the product input moisture and feed rate, as presented in Table 1. In practice, the product feed rate was adjusted by changing the set-value of the PID temperature controller regulating the exhaust drying air temperature. Additionally, two different drying pipe lengths were tested in the experiments.

For each trial, the dryer's operation was stabilized before starting the measurement. After a preheating period of 5-10 minutes, starch feeding was started until constant drying conditions were attained, i.e. when the drying air outlet temperature varied by less than +/- 1°C. This stabilization period generally took about 10 min. Once stable, an empty product collection tank was placed at the cyclone outlet and the measurements were recorded for 10-20 minutes of stable operation. At the end of the experiment, the dried product was mixed and stored in the cold room for equilibration, and sampled 48 hours later in triplicate for moisture content determination. Trials for which the final product moisture content varied by more than +/- 3% relative to the mean were excluded.

To measure the effect of a sudden change of product feed rate and test the model ability to predict the behaviour of the process in the transient phase, a specific drying trial was conducted. The drying pipe length was set to 27.2 meters, the inlet air temperature to 140 °C, the air inlet velocity to about 25 $m \cdot s^{-1}$ and the initial starch moisture was of 0.37 $kg \cdot kg^{-1} w.b.$ The operating regime of the dryer was first stabilized with the exhaust drying air temperature set to 50°C on the feeder's PID controller. After a few minutes of stable operation, the set-value of the exhaust drying air temperature was changed to 58°C at once, inducing an sudden change of product feed rate. During operation, the dried product was regularly sampled at the cyclone outlet- every 2 minutes during stable phase and about every 30s during the transient phase.

2.3. *Experimental data analysis*

2.3.1. Analysis of steady-state experiments

To evaluate the accuracy and consistency of the measurements, the water mass balance was assessed, by comparing the drying rate calculated in two different ways (i) from the product flow-rate and moisture content and (ii) from the drying air flow-rate and humidity.

The experimental data were analyzed using Matlab software (The Mathworks, Natick, MA). For the trials in steady-state operation, the measurements recorded by the data acquisition system were averaged over the trial's duration. The moisture content of the dried product, considered constant over the trial period, was calculated as the mean of the triplicate samples analysed by oven-drying method: trials for which the coefficient of variation was higher than 3% were rejected. The product flow rate, also considered constant over the trial period, was calculated based on the weight of dry product collected during the trial.

The drying air being directly heating by a LPG burner, the water released by the gas combustion had to be taken into account in the water mass balance. To this purpose, the inlet air moisture content was calculated based on ambient air humidity to which was added the water released by the LPG combustion, considering a burner efficiency of 98% and a lower heating value of 45 422 kJ/kg (gas provider specification).

Table 1.: Summary of the processing parameters of the steady-state drying experiments.

TAG	L_{pipe}	T_a^{in}	U_a^{in}	M_{st}^{in}	$\dot{m}_{st}^{in}$	Y_{in}	T_a^{out}	Y_{out}	M_{st}^{out}
	$[m]$	$[^\circ C]$	$[m \cdot s^{-1}]$	$[kg \cdot kg^{-1} w.b.]$	$[kg \cdot h^{-1}]$	$[kg \cdot kg^{-1} d.a.]$	$[^\circ C]$	$[kg \cdot kg^{-1} d.a.]$	$[kg \cdot kg^{-1} w.b.]$
1	17.2	142	11.9	0.316	77.2	0.0194	47.6	0.0525	0.134
2	17.2	141	12.0	0.317	61.8	0.0193	51.7	0.0509	0.118
3	17.2	141	11.7	0.316	55.7	0.0193	53.6	0.0496	0.099
4	17.2	142	18.5	0.332	101.5	0.0195	49.2	0.0497	0.113
5	17.2	141	18.6	0.335	91.1	0.0192	52.0	0.0471	0.099
6	17.2	142	24.1	0.325	149.8	0.0190	48.4	0.0501	0.118
7	17.2	142	24.0	0.325	135.0	0.0195	51.4	0.0488	0.107
8	17.2	141	11.9	0.390	65.9	0.0140	50.5	0.0457	0.146
9	17.2	143	12.1	0.386	60.6	0.0141	53.2	0.0464	0.136
10	17.2	141	12.1	0.381	53.9	0.0140	55.2	0.0453	0.120
11	17.2	141	12.0	0.380	50.0	0.0140	57.2	0.0440	0.113
12	17.2	183	12.2	0.314	98.8	0.0209	50.8	0.0664	0.133
13	17.2	182	12.1	0.309	77.5	0.0209	55.7	0.0630	0.096
14	17.2	182	11.7	0.321	49.0	0.0209	71.8	0.0554	0.056
15	17.2	182	19.2	0.335	143.7	0.0212	51.2	0.0645	0.123
16	17.2	181	25.0	0.368	164.4	0.0214	52.5	0.0640	0.135
17	17.2	180	25.1	0.369	152.2	0.0208	55.3	0.0621	0.119
18	20.3	140	11.7	0.340	67.4	0.0190	46.6	0.0483	0.143
19	20.3	143	11.6	0.340	56.3	0.0191	50.1	0.0472	0.114
20	20.3	141	11.8	0.340	49.2	0.0191	52.9	0.0452	0.095
21	20.3	134	20.4	0.378	82.5	0.0205	52.0	0.0452	0.122
22	20.3	133	20.3	0.362	70.4	0.0205	58.2	0.0445	0.069
23	20.3	135	20.0	0.362	59.4	0.0205	63.4	0.0434	0.085
24	20.3	141	12.1	0.376	48.5	0.0177	54.1	0.0447	0.127
25	20.3	142	11.9	0.389	53.0	0.0200	49.6	0.0483	0.178
26	20.3	145	11.8	0.389	41.5	0.0201	55.3	0.0470	0.115
27	20.3	145	11.8	0.389	36.3	0.0201	60.1	0.0449	0.106
28	20.3	146	12.0	0.389	30.0	0.0201	65.6	0.0426	0.083
29	20.3	142	18.1	0.441	73.3	0.0195	53.5	0.0478	0.166
30	20.3	141	18.3	0.440	57.1	0.0201	60.4	0.0427	0.146
31	20.3	142	24.6	0.442	94.7	0.0189	53.4	0.0464	0.160
32	20.3	143	24.4	0.441	76.7	0.0188	60.5	0.0421	0.134
33	20.3	182	19.4	0.363	167.1	0.0228	47.2	0.0682	0.190
34	20.3	182	19.6	0.363	110.5	0.0228	56.7	0.0618	0.119
35	20.3	182	19.7	0.368	137.2	0.0217	50.0	0.0647	0.159
36	20.3	182	19.9	0.368	112.6	0.0215	56.8	0.0603	0.119
37	20.3	186	12.0	0.371	55.0	0.0193	60.4	0.0565	0.088
38	20.3	183	13.3	0.388	85.8	0.0186	50.1	0.0617	0.156
39	20.3	182	21.9	0.381	116.2	0.0186	56.5	0.0606	0.107
40	20.3	178	25.9	0.382	159.0	0.0210	51.5	0.0636	0.136
41	20.3	180	25.7	0.385	129.2	0.0206	59.4	0.0586	0.101
42	27.2	142	11.5	0.362	39.1	0.0210	62.3	0.0416	0.099
43	27.2	142	11.8	0.363	28.1	0.0210	70.2	0.0353	0.082
44	27.2	142	18.0	0.347	73.6	0.0203	60.7	0.0439	0.089
45	27.2	142	17.8	0.362	51.6	0.0205	68.6	0.0380	0.078
46	27.2	142	23.7	0.367	121.7	0.0193	50.7	0.0494	0.129
47	27.2	143	23.5	0.366	95.1	0.0195	58.6	0.0448	0.098
48	27.2	182	10.8	0.394	60.0	0.0228	57.0	0.0614	0.127
49	27.2	182	19.4	0.400	90.5	0.0223	60.3	0.0587	0.108
50	27.2	182	19.0	0.396	75.8	0.0222	67.3	0.0534	0.088
51	27.2	183	24.6	0.401	143.1	0.0213	52.4	0.0647	0.147
52	27.2	186	24.9	0.400	123.1	0.0218	59.3	0.0614	0.115

2.3.2. Model fitting

The model was fitted to the experimental results by adjusting the values of two parameters, the particle diameter and the heat loss factor. The objective was to optimize the model's prediction in terms of the product final moisture content and the exhaust drying air temperature. The fitting was conducted individually for each trial, using a least-square difference criteria between the model output and the experimental measurement, as presented in equation 11. The problem was solved using the non-linear programming solver fminsearch provided by Matlab.

$$Obj = \left(\frac{X_{out}^{pred} - X_{out}}{\bar{X}_{out}} \right)^2 + \left(\frac{T_{a,out}^{pred} - T_{a,out}}{\bar{T}_{a,out}} \right)^2 \tag{11}$$

The resulting equations for the particle diameter and the heat loss factor were reintegrated into the drying model and the dataset was simulated again. The model prediction was evaluated for the product final moisture content, the exhaust drying air temperature and absolute humidity and the drying rate. The goodness of fit was expressed using the normalized root mean square error (NRMSE) and the fitness value (FV) according to equation12.

$$FV = 1 - \sqrt{NRMSE} \tag{12}$$

2.3.3. Dynamic simulations

The dynamic drying trials were simulated with the model and the output compared to the measurements. The input to the model were the product initial moisture and the time-series of feed rate, drying air inlet velocity and temperature. The wet product feed rate was derived from the weight of product recorded by the scale a the cyclone outlet, the input and output product moisture content. The starch final moisture content, measured on samples regularly made during the trials, was linearly interpolated between two samplings. The simulations were run using the raw time-series with a time step of 1 second, then the output results were smoothed to reduce the noise level and according to the sensors response time when given by the manufacturers, or to match the noise level of the sensors' measurements.

3. Results and Discussions

3.1. *Water mass balance assessment*

The water mass balance was assessed by comparing the drying rates calculated based on the air properties on the one hand, and based on the product properties on the other hand. Figure 2 illustrating the water mass balance, shows a very good agreement between both methods for the calculations of the drying rate with an RMSE of $1.43\,kg \cdot h^{-1}$. This validates the consistency of the measurements performed.

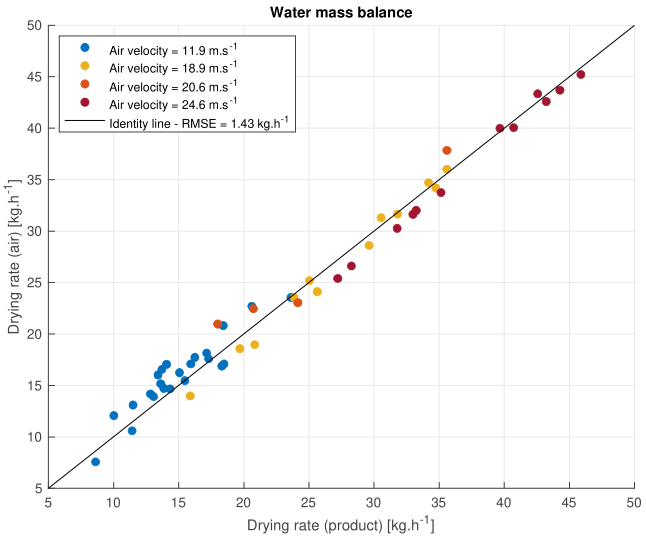

Figure 2.: Water mass balance of the steady-state drying experiments. It displays the drying rate calculated based on the product properties (x-axis) versus the drying rate calculated based on the drying air properties (y-axis). (top) Before the correction of air velocity; (bottom) after the proportional correction of air velocity.

3.2. *Analysis of fitted model parameters*

The drying model parameters, i.e. the starch particle diameter and the heat loss correction factor, were fitted individually for each drying trial. Then, we studied the variations of both parameters with respect to the operating conditions and, where appropriate, we fitted prediction equations to integrate the parameters variations into the drying model for further simulations.

Figure3 (a) illustrates the variations of the fitted particle diameter as a function of air velocity for three different values of pipe length. It ranged from 100 and 240 µm, which is consistent with actual starch particle diameters measured on pneumatic dryers [8], and showed a marked decreasing trend with increasing air velocity. To a lesser extent, particle diameter was also affected by the drying air temperature and the pipe length. The decrease of particle size with increased air velocity may be explained by the fact that higher air velocity causes more turbulence and collisions between the particles and the pipe wall, leading to disaggregation. Then, particle diameter increased with increased drying air temperature. An explanation of the agglomeration mechanisms of starch particles related to air temperature during pneumatic drying was proposed by [8]. They showed that starch particles tend to agglomerate in the first section of the drying pipe where starch is in the rubbery phase and then to disaggregate as they move along the pipe, get dryer an turn to glassy phase. When temperature is high, particles have a more rubbery and sticky characteristic, especially the particle surface, leading to more agglomeration.

Finally, the drying pipe length also affected the starch particle diameter but in an unexpected manner. Indeed, longer conveying distance was expected to cause more disaggregation and lead to smaller particle diameter, while the opposite effect was observed, as can be seen in Figure 3 (a) where this effect is particularly marked for 27.2 m length. The most likely explanation is that the last section of the drying pipe, from 16 m to the outlet, was horizontal, which might alter the transfers between drying air

starch particles compared to vertical sections. However, in absence of suitable correlations, horizontal and vertical sections of the dryer were modeled identically, using the same correlations for convective transfers.

Regarding the heat loss factor, as illustrated by the histogram in Figure 3 (b), the fitted values ranged from 1.5 to 4 for about 90% of the trials. They are disttributed around the avergae of 2.62 follwing a normal distribution pattern apart for 5 trials with significantly lower values. The variations of the heat loss factor could not be explained with regard to the operating conditions, an expected result since the heat loss factor depends essentially on the external conditions from a physical point of view.

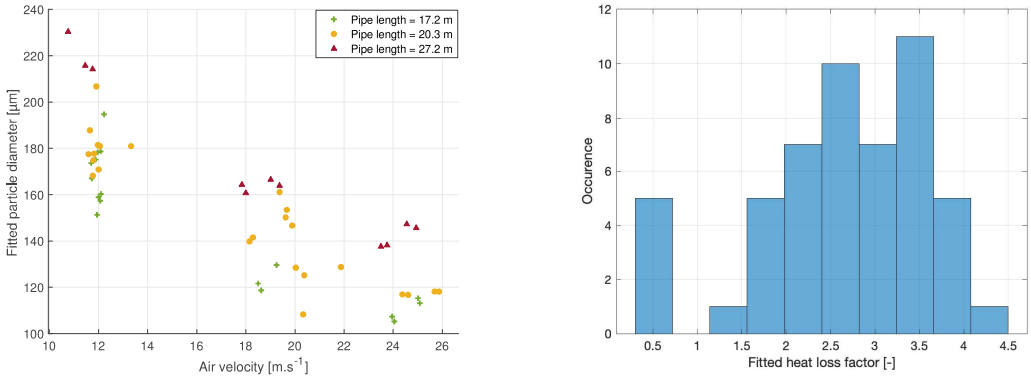

(a) (b)

Figure 3.: Fitted model parameters as a function of air velocity and drying pipe length: (a) particle diameter (b) heat loss factor, .

3.3. *Simulation of the steady-state trials*

To validate the model prediction capacity, all the drying trials were simulated with the drying model after integrating the effect of the operating conditions on particle size. To this purpose, an estimate equation of particle diameter (13) was fitted using a multivariate robust linear regression. The considered variables were the air velocity and temperature and the drying pipe length . A first -order linear model was chosen because it gave a good fit of the results with a limited number of parameters, although its physical meaning was limited. As a consiequence, it should not be used outside the considered range of air velocity, pipe length and air temperature. The fitted equation parameters are given in Table 2 and the R-squared was 0.91. For the heat loss factor, the average of fitted values, i.e. 2.62, was used, since no dependence on operating conditions was identified.

$$d_p = \alpha_0 + \alpha_1 \cdot U_{air}^{in} + \alpha_2 \cdot T_{air}^{in} + \alpha_3 \cdot L_{pipe} \tag{13}$$

The simulations results are presented in 4. It compares the model outputs to the experimental measurements in terms of the final product moisture, the air outlet moisture and temperature and the drying rate. Overall, the predicted values show very good

	Estimate	SE	T-Stat	p-value
α_0	0.000117852404472182	1.1 8245714462789e-05	9.96673790738262	2.82449470114701e-13
α_1	-5.36123276922549e-06	2.52061449039656e-07	-21.2695467301786	4.42940848644010e-26
α_2	3.53425430740599e-07	6.48000449688632e-08	5.45409236846089	1.69034103668958e-06
α_3	3.54583213548689e-06	3.54296979523827e-07	10.0080789292996	2.46680236360622e-13

Table 2.: Fitted coefficients values of the particle diameter estimate Equation 13.

agreement with the measurements with fitness values ranging from 0.91 to 0.98 for the four considered variables. The gaps between the model outputs and the measurements can be explained by the uncertainties in experimental measurements, by the natural variability of cassava starch properties and by uncontrolled external conditions which may inflence the heat losses. The discrepancies should be compared to the errors in the mass balance of the drying trials, particularly 4(d) illustrating the predicted versus calculated drying rate. It shows that the errors in the model output are of similar magnitude to those of the measured mass balance. In other words, the model prediction accuracy is comparable to the accuracy of the measurement system. As a conclusion, the model gives a reliable prediction of the process behavior in steady-state operating conditions.

3.4. *Simulation of system dynamic response*

The second validation of the model relates to its ability to predict the dynamic response of the process to variations in the operating conditions. In the present case, the response to variations in feed rate were measured and simulated. The variations of product feed rate were induced by a change of the set-value of the exhaust drying air temperature on the PID controller. The simulation results are presented in Figure 5. It shows first the variations of product feed rate and the simulated and measured response in terms of the air output temperature and moisture. For easier readability, a low-pass filter was applied to the results to limit high frequency variations. Overall, the model provided a relatively good prediction of exhaust drying air temperature and humidity variations.

For air humidity, the model was able to predict rapid variations with a high level of accuracy. The gap of air humidity level before and after the feed rate change seemed slightly underestimated, although the prediction accuracy was largely acceptable. For temperature, the model prediction showed great variations while the measurement was relatively stable, which can be explained by the thermal inertia of the drying duct that tends to stabilize air temperature and limit the peaks. This phenomenon was not taken into account in the drying model. Nevertheless, the average temperature level was very consistent with the measurement and the temperature gap before and after the change of feed rate was well estimated.

More generally, discrepancies between the model prediction and the measurement may also arise from the uncertainties in the determination of instantaneous product input mass flowrate. It was indeed calculated from the weight of dry product collected after the cyclone separator and the moisture content interpolated from spot measurements on regularly taken samples. Therefore, the possible accumulation of product in the cyclone and variations of moisture content between the samplings can lead to important errors in the determination of input product mass flow.

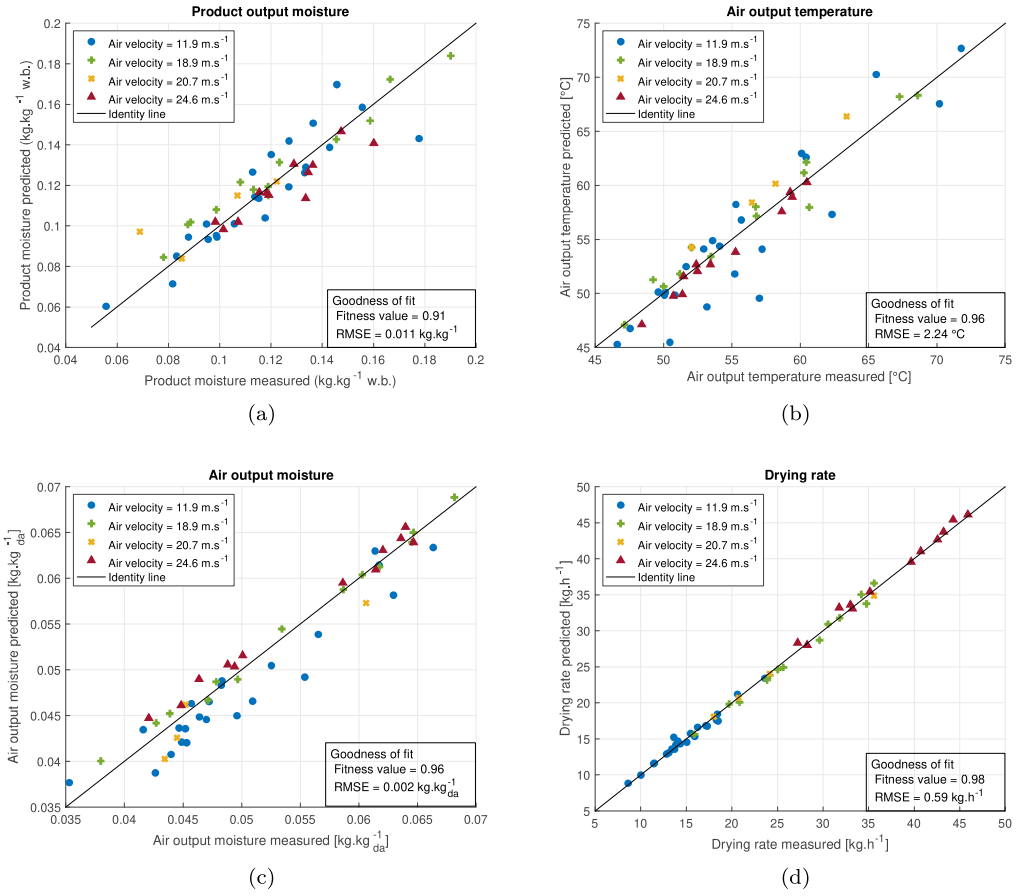

Figure 4.: Comparison of the model outputs with the experimental values. (a) Product final moisture content; (b) Air outlet temperature; (c) Air outlet absolute humidity; (d) Drying rate.

3.5. *Consequence of particle diameter variations on dryer design strategy*

A major finding of the present work is that the diameter of starch particles during pneumatic drying was greatly affected by air velocity. This has major consequences on the design strategy of pneumatic dryers. In the article we published in 2017 [4] where we first presented the pneumatic drying model, we conducted simulations to analyze the effects of pipe geometry and operating conditions and draw guidelines to optimize pneumatic dryers design with respect to energy efficiency and pipe length. At this time, in absence of detailed experimental data, the effect of air velocity on particle diameter was not identified and considered. As a result, we concluded that air velocity mainly affected residence time, therefore, increasing air velocity tended to extend the pipe length required to dry the product.

However, in the light of the results presented in this article, these conclusions should be revised. Indeed, at increased air velocity, the shorter residence time in the drying pipe is actually compensated by the smaller particle size, which has important consequences on dryer design and operation strategy. To illustrate this, we conducted simulations to calculate the processing capacity of a dryer as a function of pipe length and for several values of air velocity from 10 to 25 $m \cdot s^{-1}$. For this simulation, we

fitted a new equation for particle size estimate, function of air velocity and temperature only, Following equation 14. The effect of pipe length previously included for the model evaluation was ignored in this case since in general, pneumatic conveying dryers include only vertical upward and downward sections. The equation coefficients are given in Table 3 and the R-squared value was of 0.71.

$$d_p = \beta_0 + \beta_1 \cdot U_{air}^{in} + \beta_2 \cdot T_{air}^{in} \tag{14}$$

	Estimate	SE	T-Stat	p-value
β_0	0.000176088519652818	1.79591540664432e-05	9.80494509938201	3.85542529363887e-13
β_1	-4.87039512056137e-06	4.43032868128409e-07	-10.9933042691309	7.90990757414623e-15
β_2	3.91590121459895e-07	1.15035942105561e-07	3.40406758350845	0.00133205030519486

Table 3.: Fitted coefficients values of the particle diameter estimate Equation 14.

For the simulations, the pipe diameter was set to 150 mm, the drying air temperature to 180°C and the initial starch moisture content to 0.37 $kg \cdot kg^{-1} w.b.$ For each value of pipe length and air velocity, we calculated the starch flow rate resulting in an final moisture content of $0.125 kg \cdot kg^{-1} w.b.$ The results are presented in Figure 6, (a) illustrating the dryer's processing capacity in terms product output flow rate and (b) presenting the specific energy consumption for drying as a function of pipe lentgh. This result clearly shows that increasing air velocity allows a substantial gain in drying capacity without altering the drying efficiency, in particular for pipe lentgh higher than 15 meters. This is explained by the fact that the shorter resdience time caused by higher air velocity is compensated the smaller particle size. From 16 m pipe length and above, an air velocity of 25 $m \cdot s^{-1}$ provides the highest energy efficiency and processing capacity.

4. Conclusion

- A series of experiments was conducted on a pilot-scale dryer to produce extensive and reliable data for the validation of previously developed drying model
- The model was successfully tested on two types of data:
  - A series of averaged data from steady-state operation periods. The model was fitted by adjusting two parameters: the average particle diameter and a heat loss factor. To provide a good fit, the particle diameter needs to be adjusted to the air velocity level. The fitted particle size decreases with increased air velocity, suggesting that there is probably an effect of flow turbulence on particle attrition that is not taken into account by the model. This effect is frequently reported as a quality concern in pneumatic transport of powder.
  - Dynamic process measurements including a step-change of product feed rate. Using fixed values of the model parameters (particle size and heat loss factor), the model successfully predicted the dynamic response of the process to a step change in product feed rate. It gives a good prediction of exhaust drying air temperature and, with a higher accuracy, of exhaust drying air humidity.

- Consequences for dryer design:

5. Nomenclature

Variables

Ap [m2]
Ap' [m2] Projected area of a particle
C [kg·m-3] Volume concentration of water
Cp [J·kg-1·K-1] Heat capacity
CD [-] Drag coefficient
d [m] Particle diameter
D [m] Pipe diameter
Dws [m2·s-1] Diffusivity of water in starch
[-] Void fraction of the bed of particles
f [-] Coefficient of friction with the pipe wall
g [m·s-2] Acceleration of gravity
h [W·m-2·K-1] Convection coefficient (or specific enthalpy [J·kg-1] where specified)
Ls [J·kg-1] Net isosteric heat of desorption of water from starch
Lpipe [m] Total length of the drying pipe
[kg·s-1] Mass flow rate
pv [Pa] Water vapour pressure
psat [Pa] Saturation vapour pressure of water
[W·m-2] Heat flux from the air to the particle
[W·m-1] Heat loss through the pipe wall per meter of pipe
Qs [kJ·kg-1 of w] Specific heat consumption
r [m] Radial position within a particle
[kg·m-3] Density
S [m2] Section of the drying pipe
t [s] Time
T [K] Temperature
u [m·s-1] Velocity
Vp [m3] Volume of a particle
[kg·m-2·s-1] Water mass flux from particle to air, called drying rate
X [kg·kg-1 ds] Particle moisture content on dry basis (d.b.)
Y [kg·kg-1 da] Air moisture content on d.b.

Indices and subscript

a Moist air
da Dry air
ds Dry starch particle
i Initial state (dryer inlet)
f Final state (dryer outlet)
p Wet starch particles
v Water vapour
w Liquid water

References

[1] Howeler, R.; Lutaladio, N.; Thomas, G. *Save and Grow: Cassava. A guide to sustainable production intensification*; FAO, 2013; https://agris.fao.org/agris-search/search.do?recordID=XF2013001064.

[2] Dufour, D.; Hershey, C.; Hamaker, B.R.; Lorenzen, J. Integrating end-user preferences into breeding programmes for roots, tubers and bananas, *International Journal of Food Science & Technology* **2021**, *56* (3), 1071–1075. _eprint: https://ifst.onlinelibrary.wiley.com/doi/pdf/10.1111/ijfs.14911, https://ifst.onlinelibrary.wiley.com/doi/abs/10.1111/ijfs.14911.

[3] Sánchez, T.; Dufour, D.; Moreno, J.L.; Pizarro, M.; Aragón, I.J.; Domínguez, M.; Ceballos, H. Changes in extended shelf life of cassava roots during storage in ambient conditions, *Postharvest Biology and Technology* **2013**, *86*, 520–528. https://www.sciencedirect.com/science/article/pii/S0925521413002184.

[4] Chapuis, A.; Precoppe, M.; Méot, J.; Sriroth, K.; Tran, T. Pneumatic drying of cassava starch: Numerical analysis and guidelines for the design of efficient small-scale dryers, *Drying Technology* **2017**, *35* (4), 393–408.

[5] Kotzur, B.A.; Berry, R.J.; Zigan, S.; García-Triñanes, P.; Bradley, M.S.A. Particle attrition mechanisms, their characterisation, and application to horizontal lean phase pneumatic conveying systems: A review, *Powder Technology* **2018**, *334*, 76–105. https://www.sciencedirect.com/science/article/pii/S0032591018303279.

[6] Salman, A.D.; Biggs, C.A.; Fu, J.; Angyal, I.; Szabó, M.; Hounslow, M.J. An experimental investigation of particle fragmentation using single particle impact studies, *Powder Technology* **2002**, *128* (1), 36–46. https://www.sciencedirect.com/science/article/pii/S0032591002001511.

[7] Chapelle, P.; Abou-Chakra, H.; Christakis, N.; Bridle, I.; Patel, M.K.; Baxter, J.; Tuzun, U.; Cross, M. Numerical predictions of particle degradation in industrial-scale pneumatic conveyors, *Powder Technology* **2004**, *143-144*, 321–330. https://www.sciencedirect.com/science/article/pii/S0032591004001822.

[8] Aichayawanich, S.; Nopharatana, M.; Nopharatana, A.; Songkasiri, W. Agglomeration mechanisms of cassava starch during pneumatic conveying drying, *Carbohydrate Polymers* **2011**, *84* (1), 292–298. https://www.sciencedirect.com/science/article/pii/S0144861710009343.

[9] Rivier, M.; Moreno, M.A.; Alarcón, F.; Ruiz, R.; Dufour, D. *Almidon agrio de yuca en Colombia : Tomo 2. Planta procesadora : descripcion y planos de los equipos*; CIAT, 2001; https://agritrop.cirad.fr/481713/.

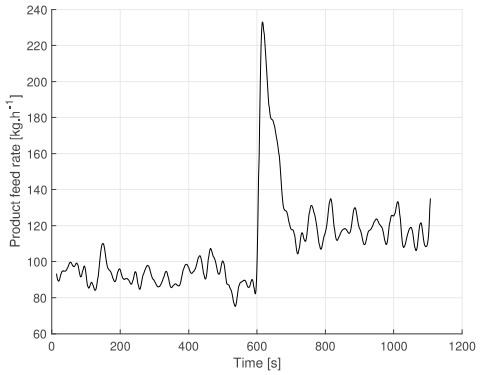

(a) Trial 1.

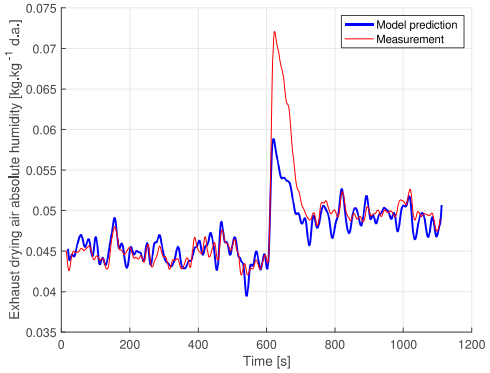

(b) Trial 2.

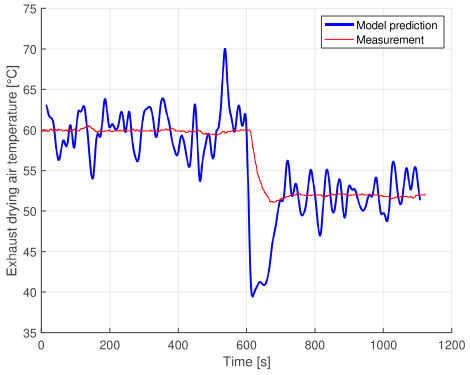

(c) Trial 3.

Figure 5.: Simulation of the dynamic response of the process to variastion of product feedrate. (a) presents the variations of product feed rate, (b) and (c) presents the evolution of the exhaust drying air moisture content and temperature respectively, and compare the measured value with the model output.

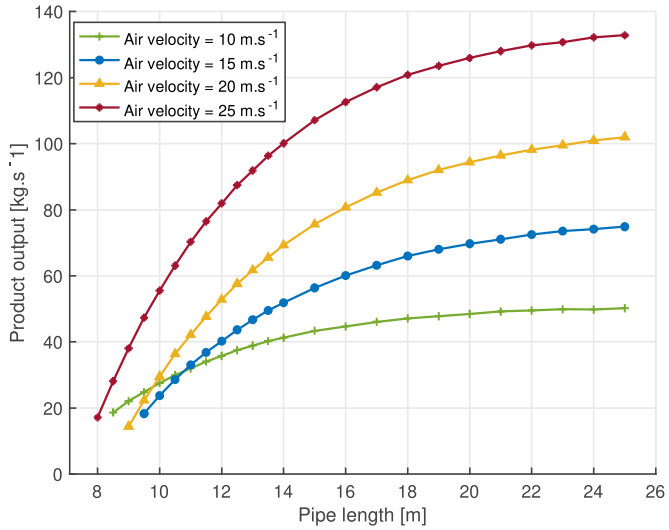

(a)

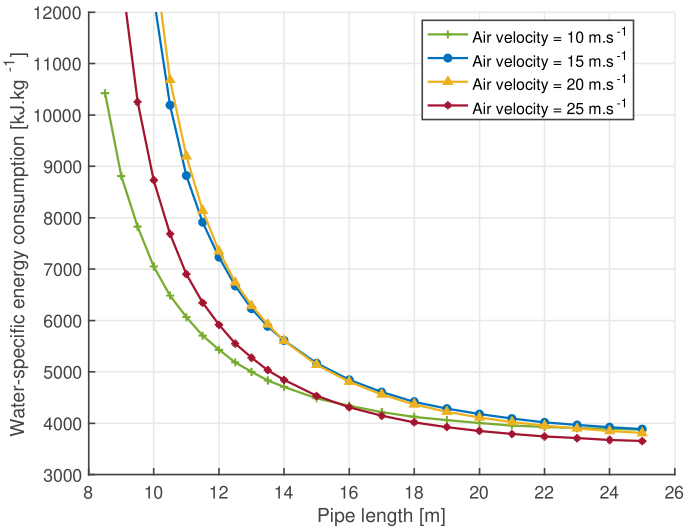

(b)

Figure 6.: Simulation results presenting (a) the drying capacity in terms product output and (b) the energy efficiency of a pneumatic dryer with a pipe diameter of 150 mm, as a function of pipe length and for several values of air velocity.